ASEAN Engineering Journal

Full Paper

# COLOR ANALYSIS IN PAPER-BASED SENSING WITH IMAGE PROCESSING AND MACHINE LEARNING ANALYSIS FOR PREDICTING CHEMICAL PROPERTIES IN LIQUID SAMPLE

Muhammad Allam Daffa Alhaqi[a], Bernadetha Grace Wisdayanti[a], Chatchawan Chaichana[a*], Napassawan Wongmongkol[a], Zulfa Hana Maulida[a], Santi Phithakkitnukoon[b]

[a]Department of Mechanical Engineering, Faculty of Engineering, Chiang Mai University, Chiang Mai 50200 Thailand.
[b]Department of Computer Engineering, Faculty of Engineering, Chiang Mai University, Chiang Mai 50200 Thailand

**Article history**
Received
05 August 2025
Received in revised form
12 November 2025
Accepted
04 February 2026
Published online
31 August 2026

*Corresponding author
c.chaichana@eng.cmu.ac.th

**Graphical abstract**

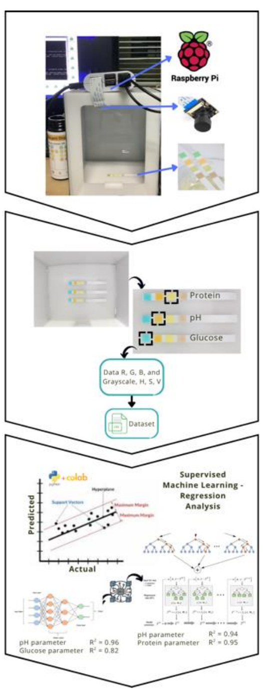


**Abstract**

Monitoring chemical properties in liquid samples, such as pH, glucose, and protein concentration, is essential in applications ranging from environmental water analysis to early-stage healthcare diagnostics. Multi-parameter test strips offer a commonly used and straightforward method for assessing these parameters in liquid samples, particularly in urine analysis. However, observer-dependent variability was noted in the interpretation of color changes, indicating potential bias among different evaluators. This study proposes a low-cost and accessible sensing method by integrating paper-based colorimetric sensing with image processing and supervised machine learning models to enhance the assessment using reagent test strips. Paper test strips were used as the medium for capturing chemical reactions., with color changes recorded using a PhotoBox equipped with a microcomputer and a Raspberry Pi camera. Extracted color features, such as Red (R), Green (G), Blue (B), Grayscale, Hue (H), Saturation (S), and Value (V) were used as inputs for predictive models, including Random Forest Regressor (RFR), Support Vector Regression (SVR), Gradient Boosting Regressor (GBR), Linear Regression (LR), K-Nearest Neighbors (KNN), and Multi-Layer Perceptron Neural Network (MLP-NN). Experimental results demonstrate that the proposed approach can accurately predict target values with strong predictive performance, achieving $R^2$ scores exceeding 0.90 in several models. Outlier handling and hyperparameter optimization were also conducted to improve prediction performance. These results suggest that this accessible and portable approach has significant potential for precise, scalable chemical assessment of multiple parameters (pH, glucose, and protein content) in liquid samples, supporting reliable monitoring in both environmental and healthcare-related applications.

*Keywords*: Colorimetric analysis, Image processing, Machine learning, Paper-based sensing, Regression analysis



## 1.0 INTRODUCTION

Water quality and purity need to be identified since traces of chemical properties can be found in any water or liquid. Some of the chemical content of water can reduce the quality of water, resulting a negative impact on environments and agriculture at high concentrations, and indicates not ideal condition. However, some elements can benefit plants in the right concentration. Several studies indicate a relationship between glucose and protein content in water and their effects on plant [1], [2], although this relationship needs further investigation to expand the applications of water sample analysis related to these parameters. Other chemical properties of water, particularly the pH level, is a crucial factor and a common parameter in water quality assessment [3]. Commonly, pH, glucose, and protein measurements are also conducted on human urine samples [4]. Thus, monitoring or assessing water quality or liquid samples is essential to ensure water quality is suitable for plant environments, supporting production and its benefits, and to enable early personal health screening related to urine sample properties and educational purposes.

Recently, there have been many reports on various methods of water quality assessment. Laboratory tests are still widely carried out due to the high accuracy values. Previous research has been conducted to determine nitrite and nitrate levels in water samples using spectrophotometric methods [5], and to determine the total hardness of water based on color change using silver nanoparticles [6]. A benchtop pH meter is commonly used to measure pH; however, its application in field or routine settings is less practical, as it requires frequent calibration with standard buffer solutions [7]. Near-infrared spectroscopy (NIRS) was employed by Tian et al. [8] to develop a method for detecting crude protein content [8], while Attia et al. [9] used NIRS to measure glucose concentration in an aqueous solution [9]. However, the laboratory assessment requires specialized tools and chemical reagents, which are often expensive and time-consuming, thereby restricting accessibility.[10]. Previous studies have developed microfluidic paper-based devices (μPADs) for the colorimetric determination of glucose using various reagents [11]; however, their complex fabrication, standardization requirements, and single-analyte focus highlight the need for simpler, multi-parameter test strips more suitable for rapid and image-based analysis.

Commercial water test kits are widely used instruments for assessing water quality. Paper-based instruments are used to assess water quality on-site based on the color displayed as a result of chemical reactions. The conventional use of water test kits requires manual observation of color matching between the reference and test strips after color changes. To avoid bias of the test result among different evaluators, digital image processing and neural networks were employed to predict parameter values more accurately. In previous studies, test strip images were captured using a smartphone camera [12], [13]. However, the image quality captured by an internal smartphone camera varies with the device's brand and model, making it inconsistent [14]. Therefore, in this study, a dedicated Raspberry Pi 5MP camera attached to the PhotoBox was used to avoid the influence of brand, model and software on the smartphone, resulting in more consistent image quality.

The Universal Indicator paper test strip is a relatively low-cost and reliable medium, especially when combined with advanced color analysis using computer vision or smartphone app color analysis. In this research, a multi-purpose test strip is proposed as a medium for testing pH, protein, and glucose. Digital image processing techniques based on computer vision can be employed to provide consistent outcomes. Furthermore, machine learning methods can be utilized in conjunction with digital image processing to support the proposed method.

This study proposes a new method for assessing aqueous solution samples using multi-purpose test strips as low-cost media for sampling. Coupled with a custom PhotoBox, colorimetric analysis using computer vision, and machine learning analysis, this approach enables users to perform multi-parameter, on-site analysis that is accessible and versatile. This method may support a variety of liquid assessment applications, from agricultural and environmental field testing to early personal health screening by urine analysis and educational purposes.

## 2.0 METHODOLOGY

This research methodology is divided into four main stages: material and sample preparation, data collection, image processing, and supervised machine learning model evaluation. Figure 1 shows an illustration of the proposed method for color analysis in paper-based sensing with image processing and machine learning. The commercial reagent test strips (URS-4K) and a custom-built device, the PhotoBox, equipped with a Raspberry Pi 3B+ microcomputer and a Raspberry Pi Camera (5MP) were used in this study for data acquisition and image processing. The PhotoBox, constructed from white acrylic, allowed limited ambient light transmission to provide stable natural illumination, while artificial lighting (e.g., LED or NIR) was not used, as it caused excessive brightness and reduced image quality. Sampling was conducted at laboratory with specific D-glucose and protein base solution to prepare water samples with controlled, measured concentrations.

### 2.1 Material and Sample Preparation

Fifteen glucose and protein aqueous samples with varying concentrations were prepared for use in this study. Pure deionized water was used as a control sample, representing zero glucose and zero protein content. The glucose solutions ranged from 0 to 1.98 g/dL, and the protein solutions ranged from 0 to 2 g/dL. Additionally, thirteen samples were prepared with pH values ranging from 4 to 9.5. Specific D-glucose and protein powders were dissolved in deionized water to create solutions with different concentrations. To generate samples with a wide range of pH levels, buffer solutions with pH values of 4, 7, and 10 were mixed in varying proportions. The resulting pH values were confirmed using an Index-1000D pH meter and recorded as target values. The commercial multi-parameter reagent strips (URS-4K, Anti-VC interference) used in this study are capable of detecting pH, protein, and glucose simultaneously. However, this study focused on analyzing each parameter separately. Each composition was tested using the same reagent test strips. The colorimetric response on the test strip indicates the concentration levels of these parameters, which can then be interpreted visually and enhanced digitally [4], [15].

### 2.2 Data Collection

The procedure for using the water test strips involved several steps. First, each test strip was immersed in the prepared water sample for approximately 2 seconds, then left for 30 seconds to allow the color to develop. The color change was initially confirmed through visual inspection to ensure proper reaction. Following this, the test strip was placed inside a PhotoBox device, and its image was captured using a Raspberry Pi camera. All images were captured under stable natural room lighting conditions throughout the experiments. To standardize the luminance of the light environment, the grayscale/luminance index ($Y = (0.2126 \times R) + (0.7152 \times G) + (0.0722 \times B)$) was used to evaluate the luminance status in the entire captured image, and the adequate luminance level was maintained at $240 \pm 2.5$ [14].

Each captured image was then saved with its corresponding target label (parameter and concentration) for further analysis. (parameter and concentration) for further analysis. Three test strips, used as replicates, were captured simultaneously in a single image acquisition. The process was repeated twice to ensure optimal image quality.

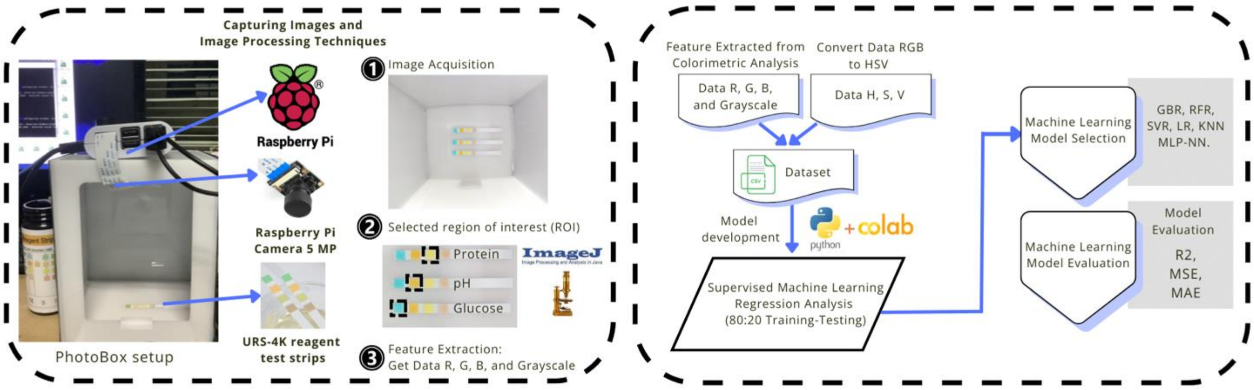


**Figure 1** Schematic diagram of color analysis in paper-based sensing with image processing and machine learning

## 2.3 Image Processing

For the digital image processing, ImageJ, an open-source software for processing and analyzing scientific images was used. A region of interest (ROI) of 50 × 50 pixels was defined to analyze the test strips image in more detail, focusing on the color pad corresponding to the specific target parameter. In this stage, color properties such as Red (R), Green (G), Blue (B), and Grayscale (Gs) values were extracted specifically from the test strip pads in each captured image. For additional color property features, the RGB values were converted to HSV (hue, saturation, value) using the OpenCV library in Google Colab. The purpose of converting the image to HSV mode was to examine the image characteristics in more detail [16] and to add more features for further machine learning analysis.

## 2.4 Supervised Machine Learning Model Evaluation

Machine learning techniques enable the development of analytical models that identify patterns and trends in water quality data. By applying these methods, underlying relationships and fluctuations in water quality parameters can be detected and interpreted. Moreover, machine learning offers predictive capabilities for anticipating changes in water quality and contaminant levels. These approaches enhance the reliability, robustness, and efficiency of the analysis process, allowing for faster and more cost-effective water quality assessment [17].

The machine learning algorithms used in this study are Random Forest Regressor (RFR), Support Vector Regression (SVR), Gradient Boosting Regressor (GBR), Linear Regression (LR), K-Nearest Neighbors (KNN), and Multi-Layer Perceptron Neural Network (MLP-NN). Linear Regression is effective for solving regression problems in small datasets. For medium-sized datasets, Random Forest offers a reliable solution. Commonly, Artificial Neural Networks are well-suited for handling large datasets, as previously discussed [18]. In this study, the GBR and MLP-NN models were highlighted. The Gradient Boosting Regressor (GBR) is an ensemble learning model that builds a sequence of decision trees, where each new tree is trained to correct the errors made by the previous ones. This boosting approach combines multiple weak learners, typically decision trees, to create a stronger and more accurate predictive model [19]. A Multilayer Perceptron is a type of supervised feedforward neural network that includes an input layer, at least one hidden layer, and an output layer, where both the hidden and output layers utilize nonlinear activation functions [18].

Google Colab, a hosted Jupyter Notebook service that requires no setup to use and provides free access to computing resources, including GPUs and TPUs, was used in this study for machine learning analysis. Additionally, this study employed the “Scikit-learn” library to implement several machine learning regression models. Meanwhile, “NumPy” was used for numerical computations and “Pandas” package was used to read and save data. Furthermore, to evaluate the performance of the machine learning models in predicting the liquid sample properties from image data, the coefficient of determination ($R^2$ score), Mean Absolute Error (MAE), and Mean Squared Error (MSE) were calculated.

$R^2$ score quantifies the quality of fit of a set of predicted output values to the actual output values. $R^2$ was chosen as the primary performance metric due to its broad acceptance in the physical sciences and its straightforward interpretability. $R^2$ represents the percentage of explained variance for the predictions and is defined as [20]:

$$R^2 = 1 - \frac{\sum_{i=1}^{n}(y_i - \hat{y}_i)^2}{\sum_{i=1}^{n}(y_i - \bar{y})^2} \tag{1}$$

The value of $R^2$ ranges from 0 to 1, where an $R^2$ of 1 indicates a perfect fit, meaning the predicted values ($\hat{y}_i$) exactly match the actual values ($y_i$) for all observations. Conversely, an $R^2$ value of 0 implies that the model fails to capture any relationship between the independent and dependent variables, and the regression line corresponds to the mean of the dependent variable, essentially forming a horizontal line.

MAE quantifies the difference between the actual and predicted values and is calculated as the mean of these differences across the dataset. MAE is calculated using the following formula:

$$\text{MAE} = \frac{1}{n}\sum_{i=1}^{n}|y_i - \hat{y}_i| \tag{2}$$

MSE helps in evaluating different regression models on a dataset, and hence helps in selecting the best-fitting model for the problem. MSE is calculated using formula:

$$\text{MSE} = \frac{1}{n}\sum_{i=1}^{n}(y_i - \hat{y}_i)^2 \qquad (3)$$

where $y_i$ is the actual value of the target variable for data instance i, and $\hat{y}_i$ is the value predicted by the model for that instance. The squared difference between $y_i$ and $\hat{y}_i$ is calculated for each data instance, and the mean is obtained by summing these squared differences and dividing by the total number of instances (n) [21].

## 3.0 RESULTS AND DISCUSSION

### 3.1 The Use of Paper-Based Sensing with Camera and Software Color Analysis

The use of paper-based sensing or water test strip paper to assess water quality was relatively quick and reliable. However, further evaluation is warranted, as the measurement ranges between concentration levels remain relatively broad. This can cause bias in semi-quantitative water quality readings. The implementation of digital image processing for quantitative liquid assessment, based on observations from the test strip paper, can provide more precise quantitative data for the related parameters. A comparison of color properties in test strip paper with color references is presented in Table 1. Interpreting the color change results of the test strips and the provided color reference using camera and software-based computational analysis offers more precise and specific values than manual observation.

**Table 1** Interpreting color change result in test strip and color reference using camera and software color analysis

| Test Strip | | | Reference color | | | Label |
|---|---|---|---|---|---|---|
| R | G | B | R | G | B | |
| pH | | | | | | |
| 177.81 | 120.96 | 51.50 | 167.55 | 115.66 | 58.48 | 5.00 |
| 176.66 | 134.16 | 52.42 | 141.05 | 100.32 | 62.29 | 6.00 |
| 169.36 | 135.08 | 58.53 | 212.57 | 186.84 | 127.30 | 6.50 |
| 135.04 | 122.07 | 58.69 | 177.66 | 160.86 | 70.37 | 7.00 |
| 116.56 | 121.41 | 75.96 | 142.76 | 138.24 | 70.81 | 7.50 |
| 77.34 | 98.05 | 88.13 | 125.34 | 132.19 | 67.49 | 8.00 |
| 67.71 | 91.53 | 87.25 | 71.62 | 92.31 | 64.35 | 8.50 |
| Glucose content | | | | | | |
| 103.76 | 205.86 | 208.23 | 77.35 | 126.54 | 137.79 | 0.00 |
| 145.62 | 178.26 | 107.35 | 148.49 | 187.69 | 159.97 | 0.09 |
| 136.69 | 96.19 | 55.71 | 130.65 | 151.56 | 89.96 | 0.27 |
| 102.76 | 62.56 | 40.58 | 130.07 | 118.13 | 63.04 | 0.54 |
| 101.15 | 60.90 | 46.27 | 121.34 | 82.53 | 53.99 | 1.08 |
| 82.03 | 46.57 | 32.89 | 94.39 | 54.19 | 48.13 | 1.98 |
| Protein content | | | | | | |
| 216.22 | 210.81 | 132.69 | 167.92 | 158.06 | 68.70 | 0.00 |
| 217.52 | 214.19 | 137.67 | 205.42 | 204.91 | 107.94 | 0.01 |
| 219.55 | 214.52 | 134.37 | 176.37 | 186.99 | 98.90 | 0.03 |
| 213.29 | 207.71 | 114.95 | 127.14 | 155.57 | 90.05 | 0.10 |
| 209.78 | 203.98 | 113.29 | 106.92 | 152.61 | 117.51 | 0.30 |
| 173.68 | 185.33 | 114.33 | 65.43 | 115.37 | 91.62 | 2.00 |

Based on Table 1, a discrepancy was observed between the color values of the labelled test strip and the reference color when analyzed using software. The reference colors listed in Table 1 were obtained from the color reference chart provided by the test strip manufacturer. Specifically, the RGB values were extracted from the printed reference color chart, which serve as the standard reference for interpreting test results. Color serves as a highly effective feature for facilitating object recognition and segmentation in images. Among various color spaces, the RGB color model is the most widely utilized in computer vision applications due to its direct correspondence with the red, green, and blue channels of the human visual system [22]. Digital photography captures light at various wavelengths to construct a color image. For instance, combining signals from the blue (~450–490 nm), green (~520–560 nm), and red (~635–700 nm) spectral bands produces what is known as an RGB image. Cameras utilizing this specific band configuration are commonly referred to as RGB cameras, designed primarily to replicate the visual perception of the human eye in a digital format [23].

### 3.2 Feature Visualization

The RGB, Gs, and HSV values extracted from the reagent pad images showed distinct distribution patterns as the concentration of the chemical parameters increased. Figure 2, Figure 3, and Figure 4 illustrate the RGB and HSV value distribution by concentration for each parameter (pH, protein, and glucose). In Figure 2, the red and green values tend to decrease with increasing pH, while the blue and hue values show a more gradual trend. Figure 3 shows that higher glucose concentration corresponds to a marked decline in Hue (H) and Value (V) values. Figure 4 shows that higher protein concentration corresponds to increased Hue (H) values and decreased average intensity ((R+G+B)/3) values. The visual distribution plots confirmed the feasibility of using these color features as input for machine learning regression models.

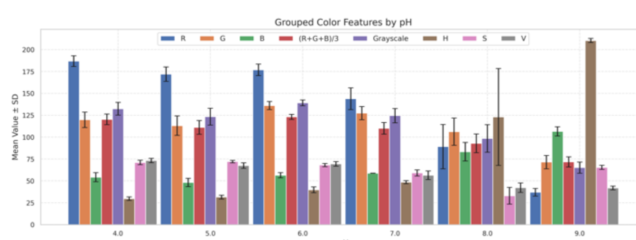


**Figure 2** Color features values versus concentration in paper-based sensors for pH parameter

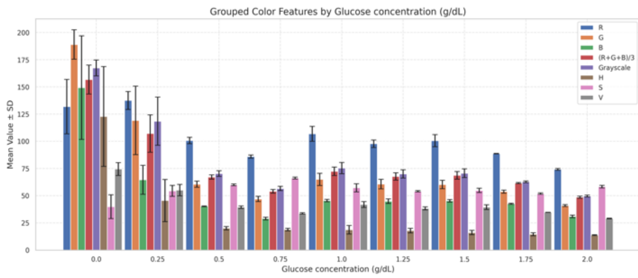


**Figure 3** Color features values versus concentration in paper-based sensors for glucose parameter

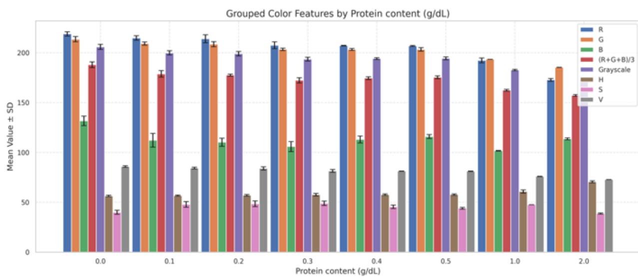


**Figure 4** Color features values versus concentration in paper-based sensors for protein parameter

The distribution of color features also highlights the importance of selecting features with the highest predictive power when training machine learning models. To assess the relevance of color features for the modeling task, correlation analysis was performed between each extracted RGB and HSV component and the actual measured concentration of pH, protein, and glucose. The correlation analysis informed the feature selection strategy used in the regression modeling phase. Figures 5, 6, and 7 show the feature importance analyzed using the GBR model in test strip for pH, protein, and glucose parameters respectively. Using GBR model, Hue (H) and Saturation (S) are the most important features in the regression modeling for this case study. The hue of a color refers to the spectral wavelength that it most closely matches. The saturation is the radius of the point from the origin of the bottom circle of the cone and represents the purity of the color [22].

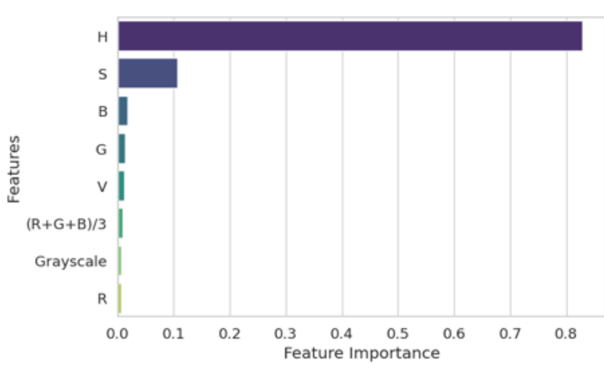


**Figure 5** Feature importance analyzed with machine learning GBR in test strip for pH parameter

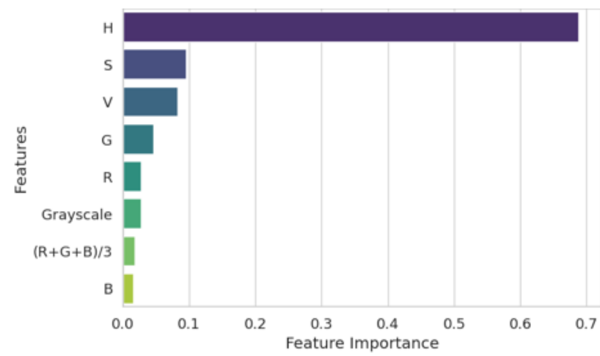


**Figure 6** Feature importance analyzed with machine learning GBR in test strip for glucose parameter

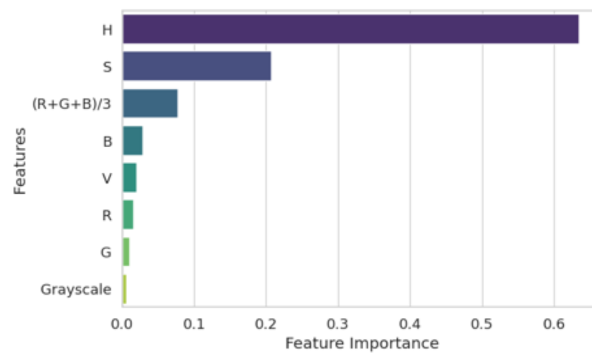


**Figure 7** Feature importance analyzed with machine learning GBR in test strip for protein parameter

## 3.3 Machine Learning Model Performance

After evaluating several machine learning regression models, MLP-NN produced the best results for the pH parameter, while GBR achieved the best results for the protein parameter. As shown in Table 2, the $R^2$ scores were close to 1, specifically 0.96 for pH (MLP-NN) and 0.95 for protein (GBR). The best model for glucose was obtained using the MLP-NN, with an $R^2$ score of 0.82. Both GBR and MLP-NN models demonstrated strong predictive performance, effectively estimating multiple parameters (i.e., pH, glucose, and protein concentrations) in liquid samples. To assess the deviation between predicted and actual values, MSE and MAE tests were performed. A summary of the model evaluation results is presented in Table 2.

The best predictive performance for the pH parameter was achieved using the GBR and MLP-NN models, with the corresponding predicted versus actual plots and error histograms shown in Figures 8–11. For the protein parameter, the top-performing models were GBR and RFR, with visualizations presented in Figures 12–15. In the glucose parameter analysis, the MLP-NN and LR models provided the best results, as illustrated in Figures 16–19.

**Table 2** Summary of regression model performance for color analysis in paper-based sensing

| Model | pH | | | Protein | | | Glucose | | |
|---|---|---|---|---|---|---|---|---|---|
| | $R^2$ | MSE | MAE | $R^2$ | MSE | MAE | $R^2$ | MSE | MAE |
| GBR | 0.94 | 0.12 | 0.24 | 0.95 | 0.01 | 0.08 | 0.78 | 0.08 | 0.18 |
| LR | 0.93 | 0.15 | 0.33 | 0.85 | 0.03 | 0.12 | 0.81 | 0.08 | 0.24 |
| RFR Regressor | 0.91 | 0.20 | 0.34 | 0.93 | 0.11 | 0.02 | 0.72 | 0.10 | 0.21 |
| KNN | 0.94 | 0.13 | 0.26 | 0.83 | 0.02 | 0.10 | 0.76 | 0.10 | 0.23 |
| SVR | 0.93 | 0.15 | 0.29 | 0.87 | 0.02 | 0.11 | - | - | - |
| MLP-NN | 0.96 | 0.10 | 0.21 | 0.83 | 0.02 | 0.11 | 0.82 | 0.07 | 0.21 |

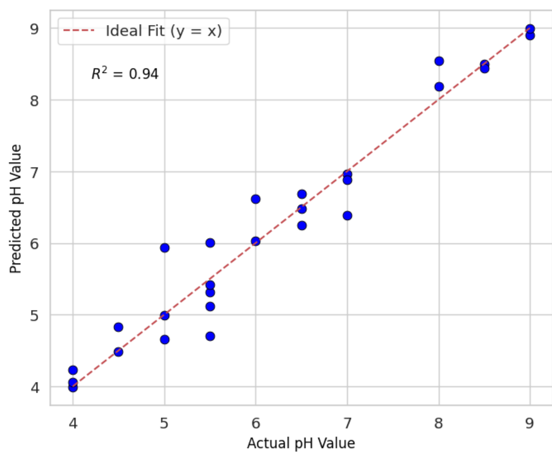


**Figure 8** visualization of predict versus actual plots in pH parameter reagent test strip using Gradient boost regressor models (GBR)

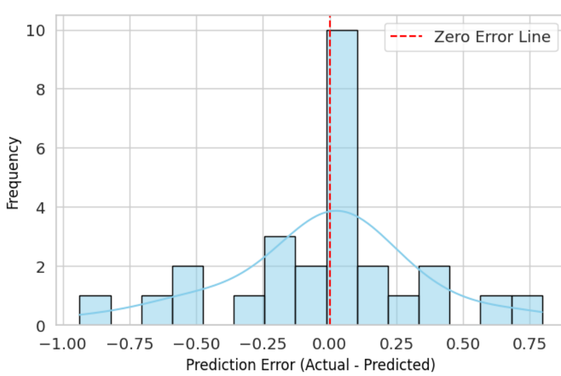


**Figure 9** histogram of prediction errors using Gradient boost regressor models (GBR)

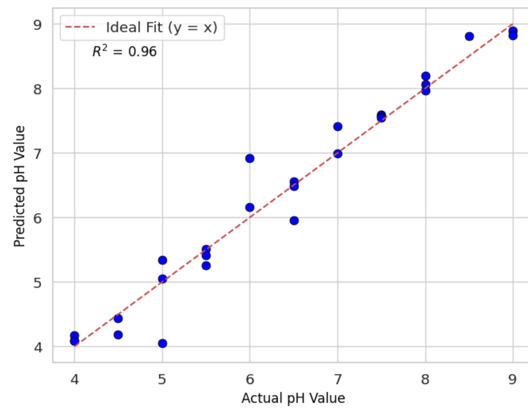


**Figure 10** visualization of predict versus actual plots in pH parameter test strip using MLP Neural Network

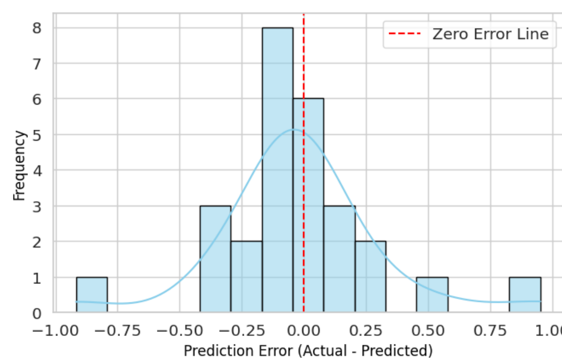


**Figure 11** histogram of prediction errors using MLP Neural Network

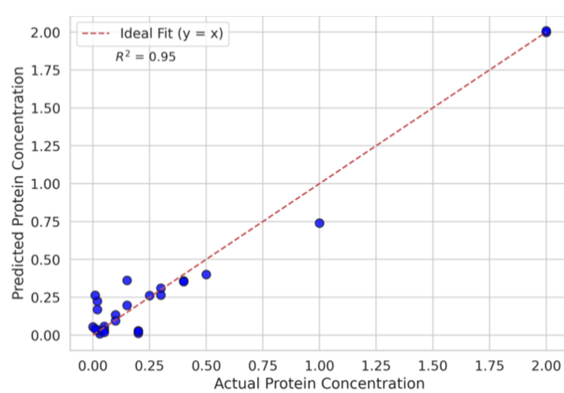


**Figure 12** visualization of predict versus actual plots in protein parameter reagent test strip using Gradient boost regressor models (GBR)

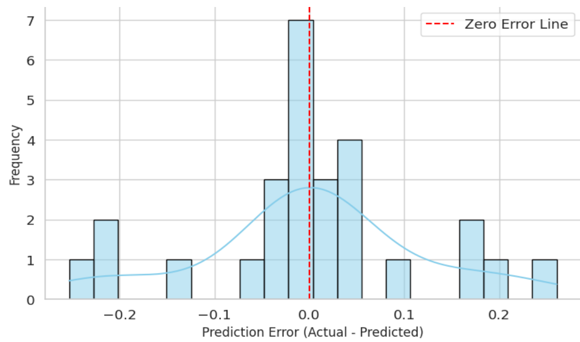


**Figure 13** histogram of prediction errors using Gradient boost regressor models (GBR)

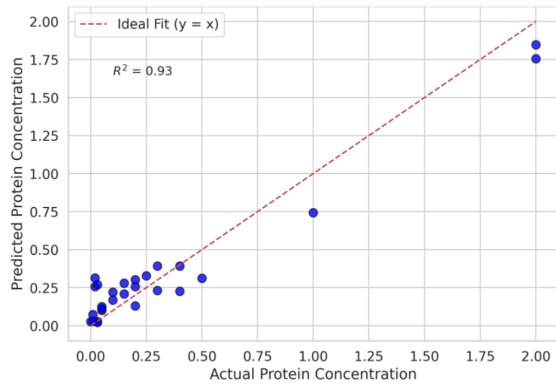


**Figure 14** visualization of predict versus actual plots in protein parameter reagent test strip using Random Forest Regressor (RFR) Regression models

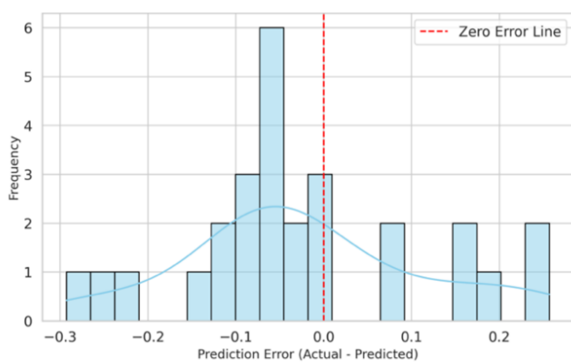


**Figure 15** histogram of prediction errors using Random Forest Regressor (RFR) Regression models

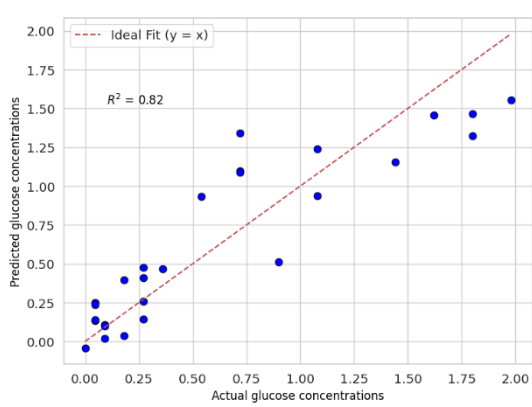


**Figure 16** visualization of predict versus actual plots in glucose parameter reagent test strip using MLP Neural Network

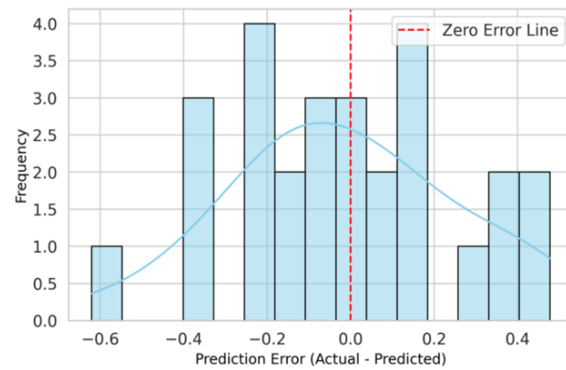


**Figure 17** histogram of prediction errors using MLP Neural Network

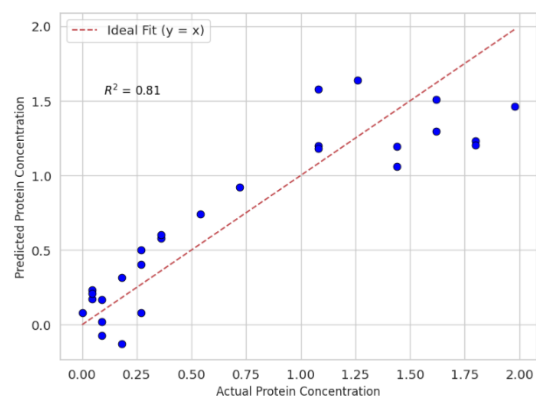


**Figure 18** visualization of predict versus actual plots in glucose parameter reagent test strip using Linear Regression (LR) model

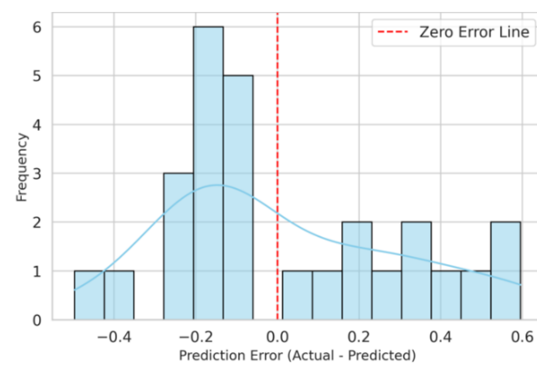


**Figure 19** histogram of prediction errors using Linear Regression (LR) model

The predicted-versus-actual plots for the best-performing model of each parameter show a strong linear trend, where most points align closely with the diagonal line, suggesting high prediction accuracy. Some mild dispersion is still observed at certain concentration levels, which could be due to weaker color differences in the test strip. This pattern reinforces that the machine learning model can capture the underlying relationship but may slightly underperform when color intensities are less distinguishable. As a baseline comparison, the prediction errors from the best machine learning model are visualized in the form of a histogram. A histogram of prediction errors shows the frequency distribution of the difference between predicted and actual values. Each bar represents how many predictions fell within a certain error range. The error distribution shows a broad spread and is centered around zero, indicating no significant bias. Overall, these results suggest that non-linear and ensemble-based machine learning models are more suitable for interpreting color features from paper-based sensors, especially when the parameter ranges and corresponding color transitions are subtle and complex. However, the observed uneven distribution of protein concentration (Figure 12 and Figure 14) is due to the test strips being primarily designed for a narrow concentration range of 0 – 0.5 g/ dL., with a significant jump in the color reference between 0.3 g/dl and concentrations above 2 g/dL. To add`ress for this, we specifically prepared samples representing 1 g/dL and 2 g/dL were specifically prepared. This limitation is acknowledged, and future studies are recommended to consider more evenly distributed concentration levels to further improve model performance.

Compared to conventional chemical testing methods, which typically involve titration, spectrophotometry, or any assays requiring laboratory-grade equipment and skilled operators, the proposed paper-based sensing approach offers a low-cost, user-friendly, and portable alternative. Traditional methods, while precise, are time-consuming and less practical for point-of-care or field-based applications. In contrast, the image-based system using a Raspberry Pi camera and reagent strips simplifies the process by capturing the color change directly and analyzing it through machine learning models. Notably, the regression models applied, particularly GBR and MLP-NN, produced high predictive performance with $R^2$ values up to 0.96 for pH, 0.95 for protein, and 0.82 for glucose, indicating a level of accuracy comparable to laboratory standards. Previous studies cited in references [4], [13], and [15] have demonstrated the potential of using smartphone-acquired images of test strips for analytical purposes, testing pH, protein, and glucose. Nevertheless, these works mainly focused on color interpretation, with limited emphasis on rigorous model performance assessment. Most of them did not include quantitative validation through metrics such as $R^2$, MSE, or MAE, which are common for evaluating predictive accuracy. Reference [12] analyzed different parameters (pH, alkalinity, total hardness, and nitrate) using reagent strips and reported an $R^2$ value of 0.8 for pH estimation using test strips and a smartphone camera. Although these prior works provide valuable groundwork for image-based analysis of test strips, their absence of comprehensive performance validation restricts their use as direct comparative benchmarks. In contrast, the present study extends beyond previous approaches by employing a standardized imaging system, utilizing a Raspberry Pi with a controlled PhotoBox setup, and implementing supervised machine learning models evaluated through robust statistical metrics, thereby enhancing both accuracy and reproducibility. This allows for a more objective and reproducible comparison across parameters (pH, protein, and glucose). This demonstrates the feasibility of the method for quantitative chemical analysis. Moreover, the compact, camera-based platform shows strong potential for portable diagnostics, especially in resource-limited settings or field applications such as agricultural water testing and preliminary health monitoring. The affordability, scalability, and ability to automate analysis without manual interpretation make this system highly relevant for the development of decentralized diagnostic tools in both environmental and biomedical domains. Specifically, for healthcare diagnostics platforms, future research should focus on validating the proposed approach using real patient urine samples with clinically diagnosed conditions to ensure medical reliability and applicability. Similar recommendations have been highlighted in recent studies emphasizing the need for clinical validation and population-specific evaluation of image-based urine analysis systems [24], [25].

### 3.4 Limitations and Future Work

This study has several limitations that should be addressed in future research. The dataset used for model training and testing was limited in both scale and diversity, as samples were generated under controlled laboratory conditions, which may not fully represent real-world variability, particularly given the different protein and glucose compositions found in various sample contexts. Additionally, the reagent strips employed were semi-quantitative and sourced from a single commercial brand, potentially introducing variability in color intensity and limiting generalizability. Future work should therefore include comparative evaluations across multiple brands with varying sensitivities and color stability to assess their influence on predictive accuracy. While RGB and HSV features were effective for regression modeling, exploring alternative color spaces or incorporating texture-based features may further enhance model robustness. Expanding the dataset to include more diverse sample conditions and potential interferences is also recommended. Moreover, integrating deep learning methods and real-time processing within embedded systems, alongside the development of user-friendly software for cloud-based or mobile deployment, could significantly improve the scalability and practicality of the proposed approach.

## 4.0 CONCLUSION

This study demonstrated the feasibility of using a paper-based colorimetric sensing approach combined with image processing and machine learning to predict chemical properties, specifically pH, protein, and glucose concentrations in liquid samples. Utilizing a Raspberry Pi camera system within a controlled PhotoBox setup, color features were extracted from reagent test strips and analyzed using RGB and HSV values. Regression modeling revealed that MLP-NN achieved the highest performance for pH and glucose prediction ($R^2$ = 0.96 and 0.82, respectively), while GBR performed best for protein prediction ($R^2$ = 0.95). These findings indicate that the proposed system can serve as a low-cost, portable, and effective alternative to conventional laboratory-based chemical testing. In addition to reducing equipment dependency and operator skill requirements, this method holds promise for point-of-care diagnostics and environmental monitoring applications. The integration of simple imaging tools with machine learning provides an accessible platform for rapid, on-site chemical analysis, supporting the development of decentralized and inclusive diagnostic technologies.

## Acknowledgement

The author would like to thank for the support from the REEC laboratory and Energy Technology and Environment (ETE) Research Center, Faculty of Engineering, Chiang Mai University, Thailand.

## Conflicts of Interest

The author(s) declare(s) that there is no conflict of interest regarding the publication of this paper

## References


[1] Li M, Yue T, Han J, Wang J, Xiao H, Shang F. 2024. Exogenous glucose irrigation alleviates cold stress by regulating soluble sugars, ABA and photosynthesis in melon seedlings. *Plant Physiology and Biochemistry*. 217: 109214. DOI: 10.1016/j.plaphy.2024.109214

[2] Boussakouran A, El Yamani M, Sakar EH, Rharrabti Y. 2024. Trend in yield and protein content relationship in a historical series of durum wheat varieties under rainfed and irrigated environments. *Crop and Environment*. 3(3): 171–176. DOI: 10.1016/j.crope.2024.05.001

[3] Jiang J, Zhang X, Wen G, Zhu M, Zheng Y. 2024. Purification Resistance Index: A new water quality assessment method toward drinking water production. *Water Research.* 267:122555. DOI: 10.1016/j.watres.2024.122555

[4] Meng R, Yu Z, Fu Q, Fan Y, Fu L, Ding Z, Yang S, Cao Z, Jia L. 2024. Smartphone-based colorimetric detection platform using color correction algorithms to reduce external interference. *Spectrochimica Acta Part A: Molecular and Biomolecular Spectroscopy*. 316:124350. DOI: 10.1016/j.saa.2024.124350

[5] Gauthama BU, Narayana B, Sarojini BK, Bello K, Suresh NK. 2020. Nitrate/Nitrite determination in water and soil samples accompanied by in situ azo dye formation and its removal by superabsorbent cellulose hydrogel. *SN Applied Sciences* 2(7): 1225. DOI: 10.1007/s42452-020-3016-5

[6] Shariati-Rad M, Heidari S. 2020. Classification and determination of total hardness of water using silver nanoparticles. Talanta. 219:121297. DOI: 10.1016/j.talanta.2020.121297

[7] Afsahi A, Ahmadi-hamedani M, Khodadi M. 2020. Comparative evaluation of urinary dipstick and pH-meter for cattle urine pH measurement. *Heliyon.* 6(2): e03316. DOI: 10.1016/j.heliyon.2020.e03316

[8] Tian Y, Sun L, Bai H, Lu X, Fu Z, Lv G, Zhang L, Li S. 2024. Quantitative detection of crude protein in brown rice by near-infrared spectroscopy based on hybrid feature selection. *Chemometrics and Intelligent Laboratory Systems.* 247: 105093. DOI: 10.1016/j.chemolab.2024.105093

[9] Attia H, Mahnashi Y, Qaid A, Mohamed NE, Qureshi KK. 2024. Near-infrared spectroscopy for glucose detection in aqueous solution. *Results in Optic*s. 16: 100738. DOI: 10.1016/j.rio.2024.100738

[10] Rostom NG, Shalaby AA, Issa YM, Afifi AA. 2017. Evaluation of Mariut Lake water quality using Hyperspectral Remote Sensing and laboratory works. The Egyptian *Journal of Remote Sensing and Space Science.* 20: S39–S48. DOI:10.1016/j.ejrs.2016.11.002

[11] Mercan ÖB, Kılıç V, Şen M. 2021. Machine learning-based colorimetric determination of glucose in artificial saliva with different reagents using a smartphone coupled <math altimg="si1.svg"> <mi>µ</mi> </math> PAD. *Sensors and Actuators B Chemical* 329: 129037. DOI: 10.1016/j.snb.2020.129037

[12] Syahputra WNH, Chaichana C, Manggala B, Wongwilai W. 2023. The Use of Neural Network Coupled with Image Processing for Water Quality Assessment (Location: Hot Spring Mae-Khachan, Thailand). *International Energy Journal.* 23(1): 47–54.

[13] Pohanka M, Zakova J. 2024. Urine Test Strip Quantitative Assay with a Smartphone Camera.Ahmed M, editor. *International Journal of Analytical Chemistry* 2024:1–8. DOI: 10.1155/2024/6004970

[14] Putra BTW, Wirayuda HC, Syahputra WNH, Prastowo E. 2022. Evaluating in-situ maize chlorophyll content using an external optical sensing system coupled with conventional statistics and deep neural networks. *Measurement.* 189: 110482. DOI: 10.1016/j.measurement.2021.110482

[15] Balbach S, Jiang N, Moreddu R, Dong X, Kurz W, Wang C, Dong J, Yin Y, Butt H, Brischwein M, et al. 2021. Smartphone-based colorimetric detection system for portable health tracking. *Analytical Methods.* 13(38):4361–4369. DOI:10.1039/D1AY01209F

[16] Hema D, Kannan DrS. 2019. Interactive Color Image Segmentation using HSV Color Space. *Science & Technology Journal.* 7(1): 37–41. DOI: 10.22232/stj.2019.07.01.05

[17] Jayaraman P, Nagarajan KK, Partheeban P, Krishnamurthy V. 2024. Critical review on water quality analysis using IoT and machine learning models. International Journal of Information Management Data Insights. 4(1):100210. DOI: 10.1016/j.jjimei.2023.100210

[18] Kotsiopoulos T, Sarigiannidis P, Ioannidis D, Tzovaras D. 2021. Machine Learning and Deep Learning in smart manufacturing: The Smart Grid paradigm. *Computer Science Review* 40:100341. DOI: 10.1016/j.cosrev.2020.100341

[19] Otchere DA, Ganat TOA, Ojero JO, Tackie-Otoo BN, Taki MY. 2022. Application of gradient boosting regression model for the evaluation of feature selection techniques in improving reservoir characterisation predictions. *Journal of Petroleum Science and Engineering* 208: 109244. DOI: 10.1016/j.petrol.2021.109244

[20] Cobb JS, Seale MA, Janorkar A V. 2021. Evaluation of machine learning algorithms to predict the hydrodynamic radii and transition temperatures of chemo-biologically synthesized copolymers. *Computers in Biology and Medicine* 128: 104134. DOI: 10.1016/j.compbiomed.2020.104134

[21] Belyadi H, Haghighat A. 2021. Supervised learning. In: M*achine Learning Guide for Oil and Gas Using Python.* [place unknown]: Elsevier; p. 169–295. DOI:10.1016/B978-0-12-821929-4.00004-4

[22] Ngadi MO, Liu L. 2010. *Hyperspectral Imaging for Food Quality Analysis and Control.* [place unknown]: Elsevier. DOI:10.1016/C2009-0-01853-4

[23] Jafarbiglu H, Pourreza A. 2022. A comprehensive review of remote sensing platforms, sensors, and applications in nut crops. *Computers and Electronics in Agriculture* 197: 106844. DOI: 10.1016/j.compag.2022.106844

[24] Kim S, Cho Y. 2022. *Predictive System Implementation to Improve the Accuracy of Urine Self-Diagnosis with Smartphones : Application of a Confusion Matrix-Based Learning Model through RGB Semiquantitative Analysis.*

[25] Kim HJ, Ph D, Kim M, Ph D, Zhang H, Kim HR, Ph D, Jeon JW, Ph D, Seo Y, et al. 2025. *Artificial Intelligence in Diagnostics : Enhancing Urine Test Accuracy Using a Mobile Phone – Based Reading System.* :178–184.